strated for lower burnups. Tests are being conducted to demonstrate full burnup at operating temperatures.

9) The aforementioned fuel concept when it incorporates the feature of vapor transport within the pin may provide for a simpler high-burnup reactor control.

10) Nuclear aircraft with gross weights in the range of 1 to 2 million pounds may be capable of payload capacities in the range of 10 to 25% of the gross weight for altitudes up to 36,000 ft and Mach numbers of 0.8.

References

[1] Wild, J. M., "Nuclear Propulsion for Aircraft," *Astronautics and Aeronautics*, Vol. 6, No. 3, March 1968, pp. 24–30.

[2] Rom, F. E. and Finnegan, P. M., "Will the Nuclear-Powered Aircraft be Safe?" *Astronautics and Aeronautics*, Vol. 6, No. 3, March 1968, pp. 32–40.

[3] Rom, F. E., Finnegan, P. M., and McDonald, G. E., "Very-High-Burnup Vapor-Transport Fuel-Pin Concept for Long-Life Nuclear Reactors," TN D-4860, 1968, NASA.

[4] Blake, L. R., "Achieving High Burn-up in Fast Reactors," *Journal of Nuclear Energy, Part A and B, Reactor Science Technology*, Vol. 14, April 1961, pp. 31–48.

[5] Blake, L. R., "Irradiation of Uranium-Metal and Uranium-Oxide Fuel Pins to High Burn-up at High Temperature," *Journal of Nuclear Energy, Part A and B, Reactor Science Technology*, Vol. 15, 1961, pp. 140–159.

[6] Morris, R. E., "Creep-Rupture Data for Welded N-155 Tubes," TN D-5195, 1969, NASA.

JANUARY 1971 J. AIRCRAFT VOL. 8, NO. 1

Evaluation of Heat Transfer for Film-Cooled Turbine Components

DARRYL E. METZGER*

Arizona State University, Tempe, Ariz.

AND

DARRELL D. FLETCHER†

AiResearch Manufacturing Company, Phoenix, Ariz.

Film cooling has been shown to be an effective method for the cooling of a variety of gas turbine engine components. In many of these applications, the region of primary interest, as far as calculation of heat-transfer rates is concerned, is the region immediately downstream of the injection location. Conventional methods for predicting heat-transfer rates, based on adiabatic wall temperature data alone, are generally inadequate in these regions. An experimental apparatus that can be used to readily obtain the comparative film cooling performance of different injection configurations, with surface heat transfer, is described. A convenient means of presenting comparative performance is used to present the results of an extensive series of tests with film injection through flush two-dimensional slots and through single spanwise lines of flush circular holes. Injection angles of 20° and 60° are covered for both injection types over a range of injection rates and downstream distances of interest in turbine cooling applications. In all cases the cooling protection provided by injection through holes is much less than that available with spanwise continuous slot injection. The results should provide the designer with a measure of the coolant penalty accrued when structural or other constraints preclude continuous injection slots.

Nomenclature

A = heat-transfer area
c_n = center-to-center distance between adjacent holes (Fig. 5)
C = surface block thermal capacity
d_n = hole diameter (Fig. 5)
G = mass flow rate per unit area
G^* = mass velocity ratio [Eq. (4)]
h = heat-transfer coefficient
l = cooled surface length
t = temperature
$\dot{q}$ = heat-transfer rate
s = actual or equivalent slot width
x = distance along the surface downstream from the injection opening (Fig. 2)
β = injection angle (Fig. 2)
θ^* = temperature difference ratio [Eq. (5)]
θ^*_{ad} = adiabatic temperature difference ratio [Eq. (6)]
μ = viscosity
τ = time
Φ = normalized average surface heat transfer [Eq. (3)]
Φ_0 = normalized average surface heat transfer at $t_f = t_m$

Subscripts

aw = adiabatic wall
f = film flow, identifies quantities evaluated at the injection nozzle exit
m = main flow, identifies quantities evaluated upstream of injection
w = wall, identifies quantities evaluated at the cooled surface

Presented as Paper 69-523 at the AIAA 5th Propulsion Joint Specialist Conference, Colorado Springs, Colo., June 9–13, 1969; submitted June 19, 1969; revision received March 11, 1970. At the Conference, E. R. G. Eckert, R. J. Goldstein, and D. R. Pedersen presented a written comment on this paper; it also is published in this issue of *Journal of Aircraft*.

* Associate Professor, Mechanical Engineering Department; also Consultant to AiResearch Manufacturing Company, Member AIAA.

† Engineer, Preliminary Design Section.

I. Introduction

FILM cooling usually describes a situation in which a secondary fluid is injected at discrete locations into a boundary-layer flow of primary fluid along a surface. The problems associated with air injection into a turbulent air boundary layer have been under almost constant investigation[1–7] since the early work of Wieghart.[8] Much of the incentive for these studies has been provided by the prospects of film cooling as a practical method for cooling gas turbine engine components. A typical example, although by no means the only one, is depicted in Fig. 1, which shows a schematic of a gas turbine nozzle vane which is film cooled in the trailing-edge region. The coolant is usually relatively cool compressor discharge air which has bypassed the combustor. The geometry of the thin trailing-edge region usually precludes adequate cooling by internal convection alone, and some of the coolant is injected into the hot gas boundary layer to reduce the surface heat flux.

The amount of surface heat flux reduction obtainable with different combinations of injection rates, geometries, and temperatures must be known before a rational design resulting in minimum coolant expenditure is possible. Surface heat-transfer rates in the presence of secondary injection are commonly evaluated by using the temperature of an adiabatic surface downstream of the injection site together with a heat-transfer coefficient associated with the primary flow alone

$$\dot{q}/A = h(t_{aw} - t_w) \tag{1}$$

The heat-transfer coefficient h is determined from Eq. (1) with measured values of heat flux and temperatures for the case of no secondary injection. Thus, the heat-transfer rates with injection are determined with a minimum of information beyond the primary stream heat-transfer characteristics; namely, adiabatic wall temperature distributions in the presence of injection. For this reason, much of the film cooling literature deals with the determination of adiabatic wall temperatures, usually presented in terms of the film cooling effectiveness η

$$\eta = (t_{aw} - t_m)/(t_f - t_m) \tag{2}$$

Correlations of effectiveness together with Eq. (1) are adequate for predicting surface heat-transfer rates only far downstream of the injection site (usually at least 40 injection slot widths downstream), even when the injection geometry is a continuous spanwise two-dimensional slot and the angle between the primary and secondary velocities is small at injection. This excludes the region immediately downstream of the injection location, which is the region of interest in many practical situations. In this near region the injection of the secondary fluid, even if two-dimensional, can significantly alter the flow pattern from that of the primary flow alone, and the effective heat-transfer coefficients may be either increased or decreased, depending on the amount and nature of the injection.

The complexity of the flow pattern is obviously increased with three-dimensional injection configurations such as hole arrays and interrupted slots as shown in the vane of Fig. 1. Unfortunately, the unique structural and aerodynamic constraints present in gas turbine components very often dictate the use of some type of interrupted injection. The need for more specific information on these types of injection geometries is apparent, and a recent paper by Goldstein et al.,[9] treats the problem of adiabatic wall temperature distributions downstream of a single circular injection hole.

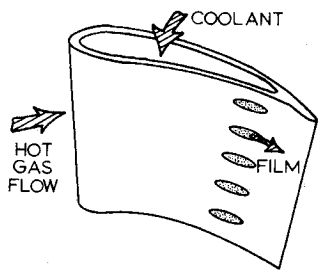

Fig. 1 Schematic of film-cooled vane.

An experimental program, designed for rapid assessment of the relative characteristics of various film cooling schemes, with surface heat transfer and in regions close to the injection location, is described. Initial results of this program have been reported[10] for the case of injection through flush, angled slots into the turbulent boundary layer on a flat, uniform temperature surface. The present paper presents results for the case of injection through single spanwise lines of angled circular injection holes and compares their heat-transfer characteristics with expanded results for the flush angled slot configuration. Figure 2 depicts the two injection types.

II. Basic Considerations and Definitions

For surfaces cooled as in Fig. 2, it is expected that the local heat-transfer rates downstream of the injection location would be influenced by the mainstream velocity and properties; the secondary fluid velocity and properties; the temperatures t_m,t_f, and t_w; the injection geometry; and the downstream distance x. For interrupted geometries, such as the present hole injection, a spanwise variation in surface heat flux at a given x station is also expected. In the present study, average surface heat-transfer rates were measured over finite x distances l, downstream of injection. These rates are compared to the heat-transfer rate measured with the same surface and mainstream conditions in the absence of any injection slots or holes. The ratio of average surface heat transfer with injection to that without injection Φ is presented nondimensionally as

$$\Phi = \Phi(G^*,\theta^*,l/s, \text{geometry}) \tag{3}$$

where

$$G^* = G_f/G_m \tag{4}$$

$$\theta^* = (t_f - t_m)/(t_w - t_m) \tag{5}$$

G_f and G_m are the mass flow rates per unit area of the film and mainstreams, respectively, and s is the actual width of a two-dimensional injection slot or the width of an equivalent slot of equal discharge area for the case of hole injection.

The functional relationship implied in Eq. (3) can be obtained[10] from a nondimensionalization of the governing boundary-layer momentum and energy equations and appropriate boundary conditions for two-dimensional slot injection, uniform surface temperature, and small temperature differences. The assumption of small temperature differences is consistent with a linear formulation of the energy problem where film cooling $t_m > t_f$ and film heating $t_f > t_m$ are similar problems governed by the same equations and boundary conditions. Thus film heating experiments can be used to

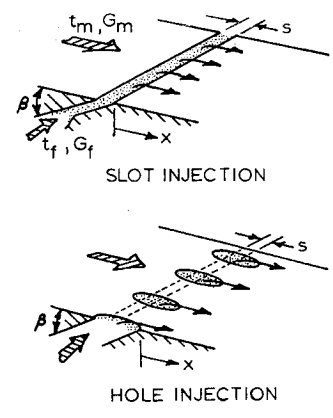

Fig. 2 Injection geometries.

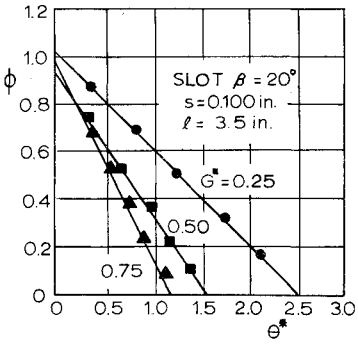

Fig. 3 Typical $\Phi - \theta^*$ results.

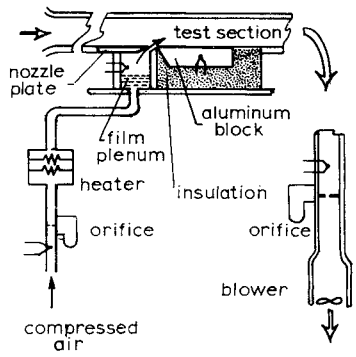

Fig. 4 Schematic of apparatus.

model film cooling problems, as is the case in the present study and in the majority of previous investigations.

Geometric modeling is explored in the present study by conducting all tests at two different values of slot width or equivalent slot width s. The geometry of the hole injection configuration is characterized by the hole diameter d_n, the center-to-center hole spacing c_n, and the injection angle β. The geometry of the film-cooled surfaces on turbine vane sets is modeled in this study with a plane heat-transfer surface in a constant cross-sectional area flow passage. The relative sizes of the tunnel cross section and injection slots and holes were chosen to correspond to prototype values.

The absence of both Reynolds number and Prandtl number in Eq. (3) does not indicate a lack of dependence of surface heat-transfer rate on either of these parameters, but it does imply that their effect on the normalized heat transfer Φ is much less important than those of the independent parameters listed. In the present study, the mainstream Reynolds number $G_\infty l/\mu$ was varied by changing both the mainstream velocity and surface length, but an extensive independent variation was not made. For slot injection, the tests indicate that the results can be adequately correlated independently of Reynolds number, but in the case of hole injection more work is needed to explore this effect. The effect of Prandtl number was not investigated in the present study. All tests were conducted with air as both the primary and secondary fluid with temperatures within 25° F of ambient levels.

Typical values of Φ obtained in the present study are shown in Fig. 3 as functions of G^* and θ^* for injection through a 0.1-in. slot at $\beta = 20°$ over a surface length of 3.5 in. When $\theta^* = 0, t_f = t_m$ and the value of Φ at this point indicates the hydrodynamic effect of the film on the downstream surface heat transfer. Figure 3 demonstrates that for slot injection at 20°, this effect, averaged over a surface length 35 slot widths long, is quite small for $0.25 \leq G^* \leq 0.75$.

When $\Phi = 0$, the average surface heat-transfer rate is zero, although in general the local rates on the surface will not be zero. If the value of θ^* when $\Phi = 0$ is denoted by θ^*_{ad}, then

$$\theta^*_{ad} = (t_f - t_m)/(t_{aw} - t_m) \tag{6}$$

Here t_{aw} must be interpreted as the surface temperature corresponding to zero average surface heat flux. The inverse of θ^*_{ad} has the form of film cooling effectiveness, although it must be emphasized that the actual surface condition is not locally adiabatic. Nevertheless, the value of θ^*_{ad} for a given configuration and flow is a measure, like the conventional effectiveness, of the mixing between the primary and secondary streams.

Thus, the value of θ^*_{ad} conveys essentially effective information, whereas the value of Φ at $\theta^* = 0$ indicates effects of injection on heat transfer that are not available from adiabatic wall temperature distributions alone. A value of Φ at $\theta^* = 0, \Phi_0$, equal to unity, indicates that the average surface heat flux can be accurately predicted by Eq. (1), and the percent increase or decrease in Φ_0 from unity is directly proportional to the error incurred in predicting surface heat flux from Eq. (1) and measured adiabatic wall temperatures alone.

The linearity of the measured $\Phi - \theta^*$ values apparent in Fig. 3 is a consequence of the linear governing energy equation and is expected for the small temperature differences of this study.

III. Apparatus and Procedure

The experimental data were acquired with a novel transient test facility which substantially reduces the testing time compared to more conventional steady-state experiments and makes feasible the evaluation of the relative performance of a wide variety of possible alternative injection designs.

The experiments were conducted with a small, constant cross-sectional area, open cycle wind tunnel as shown in the schematic of Fig. 4. The main-stream air is induced from ambient laboratory conditions through the 2 in.-by-0.5-in. test section by means of a downstream axial blower. The blower passes both the mainstream (100–150 lbm/hr) and film stream (2.5–27 lbm/hr), and the combined flows are metered with a standard orifice located upstream of the blower. The secondary air is supplied from the laboratory compressed air system through an electrical heater and another standard orifice to the injection section, built into the tunnel floor. The injection section consists of a plenum chamber with baffles and screens topped by removable nozzle plates that provide the different injection configurations. The nozzle plates are all 0.250 in. thick and 4.15 in. long, machined from acrylic plastic.

A total of eleven nozzle plates were used: four slot nozzles with $s = 0.050$ in. and 0.100 in. at 20° and 60° injection angles; four hole nozzles at $c_n/d_n = 1.71$ with $s = 0.050$ in. and 0.100 in. at 20° and 60° injection angles; and three hole nozzles at $c_n/d_n = 1.55$ with $s = 0.050$ in. and 0.100 in. at 20° and 60° injection angles.

The nozzle plates mount flush against the interchangeable heat-transfer surfaces, which are aluminum blocks of various lengths in the flow direction, 1.5 in. wide and 1.0 in. deep. Seven surfaces were used ranging in equal 0.5-in. increments from 0.5 in. to 3.5 in. long. This provides for average heat-transfer rate measurements over downstream distances $5 \leq l/s \leq 35$ for the 0.100-in. nozzles and $10 \leq l/s \leq 70$ for the 0.050-in. nozzles.

The relationship between the nozzle plates and heat-transfer surfaces is illustrated by the top view of the tunnel floor shown in Fig. 5. The holes in the hole nozzles were spaced so that the edges of the heat-transfer surface were directly downstream of a hole centerline in order to minimize end effects. The hole nozzles corresponding to the 0.050-in. equivalent slot width have a total of 9 and 11 holes; those with the 0.100-in. width have 5 and 6 holes. A sandpaper trip is used on the tunnel floor upstream of the nozzle plates. The heat-transfer rates measured on all of the test surfaces without film injection (nozzle plate without openings used) correspond to those expected for a turbulent boundary layer.

The heat-transfer rates both with and without heated injection are determined by establishing the flow(s) at steady

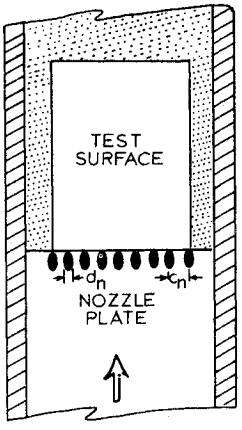

Fig. 5 Top view of test surface and nozzle plate.

values of velocity and temperature while heating the aluminum test surface block to a temperature in excess of the desired maximum test value. Heating is stopped, and the transient cooling of the block in the presence of the film is recorded on a self-balancing potentiometric recorder.

The aluminum blocks that form the test surfaces have negligible internal thermal resistance in comparison with the convective thermal resistance at the upper surface of the block. This establishes a spatially uniform temperature distribution throughout the block at all times during the cooling transient. Equating the heat loss through the block surfaces to the loss in internal energy of the lumped block thermal capacity C results in the following expression for the average convective heat-transfer rate $\dot{q}$ on the test surface:

$$\dot{q} = -C(dt_w/d\tau) - \text{correction term} \qquad (7)$$

where the correction term accounts for the finite conductance of the insulation surrounding the block on five sides. This undesired heat leakage is determined by auxiliary testing with the top surface of the block insulated. Additional details of the experimental apparatus, including the determination of the correction term in Eq. (7) have been previously reported.[10,11]

During a transient test with secondary injection, all the flow variables, including t_f and t_m, are maintained constant; so, at any given time during the transient, the value of t_w measured and the value of $\dot{q}$ calculated from Eq. (7) correspond to a single value of θ^*. This calculated heat-transfer rate is normalized with the rate observed for the same mainstream conditions and surface temperature in the absence of injection, and the results are presented as in Fig. 3. The data points shown in this figure correspond to values of t_w during the transient at which the $t_w - \tau$ derivative is evaluated from the recorded block temperature response. The appearance of the expected linear $\Phi - \theta^*$ relationship serves as a check on the experimental and numerical data reduction procedures used.

The value of Φ at $\theta^* = 0, \Phi_0$, can be obtained by extrapolation or by conducting a separate transient test with the film

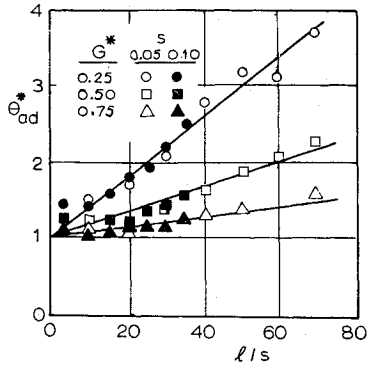

Fig. 6 θ^*_{ad} for slot injection at 20°.

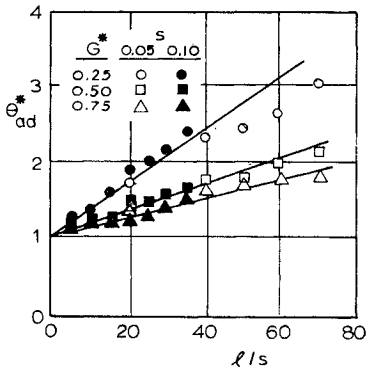

Fig. 7 θ^*_{ad} for slot injection at 60°.

temperature equal to the mainstream temperature. In the present study both methods were used, and in all cases the extrapolated $\theta^* = 0$ results were found to be in excellent agreement with the actual $\theta^* = 0$ tests. To further verify the validity of this transient evaluation procedure, comparative steady-state tests have been conducted and reported.[10] The two sets of results are in excellent agreement.

IV. Results and Discussion

Slot Injection

Throughout the test program, the cooling transients were evaluated as described in the previous section at from 5 to 7 values of t_w between $\theta^* = 0$ and θ^*_{ad} to establish the characteristic lines as shown in Fig. 3. In all of the following presentation, the film-cooling performance at various combinations of the independent parameters will be specified in terms of the intercepts of these lines, Φ_0 and θ^*_{ad}.

Figure 6 shows the effects of G^* and l/s on θ^*_{ad} for the continuous slot injection at $\beta = 20°$. The agreement between the 0.050-in. slot and 0.100-in. slot results is, in general, quite good. Experimental uncertainties have been estimated by the methods of Kline and McClintock,[12] and uncertainties of $\pm 6\%$ in the determination of heat flux lead to estimated uncertainties of $\pm 8\%$ in the value of Φ_0, and $\pm 7\%$ to $\pm 10\%$ in the value of θ^*_{ad}. The indication of a θ^*_{ad} intercept of unity for $l/s = 0$ is to be expected, since with continuous slot injection the initial surface edge is completely covered by the unmixed film.

Similar results were obtained with the 60° slot injection except that high G^* performance in this case is not as good as before, as indicated in Fig. 7 for $G^* = 0.50$ and 0.75 results. The relatively linear θ^*_{ad} vs l/s behavior suggests a simple correlation of these results. Figure 8 shows this correlation for the $\beta = 20°$ results of Fig. 6. The best-fit line through the data is given as

$$\theta^*_{ad} = 1.0 + 0.00619G^{*-1.35}(l/s) \qquad (8)$$

for the ranges $0.25 \leq G^* \leq 0.75$, $0 \leq l/s \leq 70$, and $\beta = 20°$.

A similar correlation has been obtained for the $\beta = 60°$ results of Fig. 7, and has about the same appearance as Fig. 8.

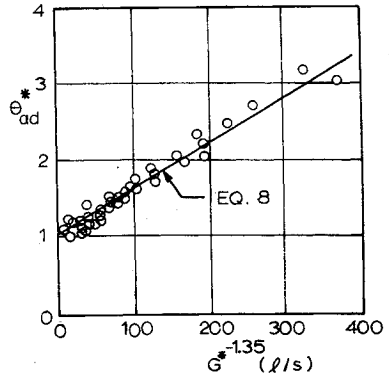

Fig. 8 θ^*_{ad} correlation for slot injection at 20°.

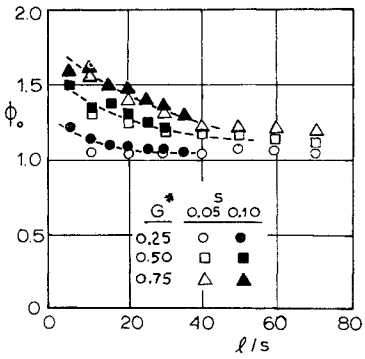

Fig. 9 Φ_0 for slot injection at 60°.

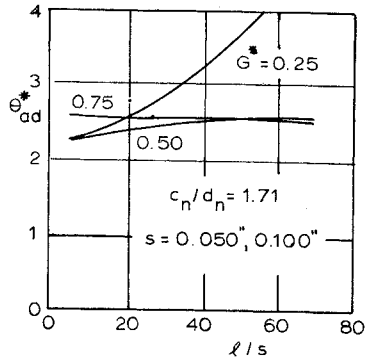

Fig. 11 θ^*_{ad} for c_n/d_n = 1.71, 20°.

The graph is omitted here for brevity, but the best-fit line is given as

$$\theta^*_{ad} = 1.0 + 0.01155G^{*-0.75}(l/s) \quad (9)$$

for the ranges $0.25 \leq G^* \leq 0.75$, $0 \leq l/s \leq 70$, and $\beta = 60°$.

The differences between 20° and 60° injection apparent in Figs. 6 and 7 are those differences that would be revealed by adiabatic wall results with high values of θ^*_{ad} corresponding to low values of effectiveness and visa-versa. Additional insight into the effects of injection is provided by the presentation of the influence of G^* on Φ_0 over various surface lengths l/s. Figure 9 shows this influence for $\beta = 60°$. Again there is good correspondence between the results for the two different widths at similar values of l/s. The effect of the film in raising the average effective heat-transfer rate is small for $G^* = 0.25$ except very close to the slot; however, for the larger values of G^* the effect is significant over at least the first thirty slot widths downstream.

The implication of a value of Φ_0 equal to 1.5 is best demonstrated as follows. For a prototype application where surface heat flux reduction but not reversal is required (net heat transfer into the surface, $\Phi > 0$ and $\theta^* < \theta^*_{ad}$), the actual heat-transfer rate into the surface is 50% greater than that predicted from measured values of effectiveness and use of primary flow heat-transfer coefficients. For a similar application where heat flux reversal is required (net heat transfer out of the surface despite $t_m > t_w$, $\Phi < 0$, and $\theta^* > \theta^*_{ad}$) the actual heat-transfer rate out of the surface is 50% greater than the value predicted similarly.

The corresponding values of Φ_0 determined from the slot injection tests at $\beta = 20°$ are omitted here because of their relatively uninteresting behavior. With few exceptions, the values of Φ_0 obtained with $\beta = 20°$, at all values of G^* and l/s, were equal to unity within the experimental uncertainty. This is true not only with slot injection but was observed for the hole injection results of the present study as well.

Hole Injection

The behavior of θ^*_{ad} for hole injection for both values of c_n/d_n tested differs considerably from that observed for the continuous slot results. First, the values do not extrapolate to $\theta^*_{ad} = 1.0$ at $l/s = 0$ as is the case for the slots. Instead, they extrapolate back to from approximately 1.5 to 2.6, depending on the particular nozzle and injection rate. Secondly, at small values of l/s, the larger injection rates result in higher values of θ^*_{ad}. At larger values of l/s, the opposite effect persists with larger injection rates resulting in lower values of θ^*_{ad}. The crossover distance is in the vicinity of 20 equivalent slot widths. These trends are illustrated for $\beta = 20°$ in Figs. 10 and 11 for $c_n/d_n = 1.55$ and 1.71, respectively. The agreement between the 0.050-in. equivalent slot results and the 0.100-in. results is not as good in these tests as it was with the slots; the difference is as large as 20% in some cases. This scatter in the data, coupled with the aforementioned reversing effect of G^*, serve to make a graphical presentation of results confusing. Figures 10 and 11 and subsequent figures for the hole injection results show, instead, faired lines that represent the individual data points to within ±10% in all cases.

Again, values of Φ_0 are not presented for these 20° results because of their proximity to unity in all cases.

Figures 12 and 13 present the hole injection results for $\beta = 60°$. The θ^*_{ad} results in Fig. 12 are very little different than the corresponding 20° results for $G^* = 0.25$. However, the film performance is considerably poorer for $\beta = 60°$ for the higher values of G^*. For $\beta = 60°$ only one nozzle with $c_n/d_n = 1.55$ was constructed and used in the tests, and the results for this one as well as those from the two $c_n/d_n = 1.71$ nozzles are equally well represented by the faired lines of both Figs. 12 and 13. The Φ_0 results of Fig. 13 are very similar to those of the 60° slot injection shown in Fig. 9, and the implications of large values of Φ_0 are the same except that one must remember that the hole results are spanwise-averaged values of quantities that undoubtedly have large spanwise variations.

A final interesting comparison is shown in Fig. 14 for the practically important case of injection through holes at $G^* = 0.25$. The data points are from all the hole injection tests at $G^* = 0.25$ for $\beta = 20°$ and 60°, $c_n/d_n = 1.55$ and 1.71, and $s = 0.050$ in. and 0.100 in. The values and trends of these results are all very similar and considerably higher than what could be expected from continuous slot injection, represented by the solid line.

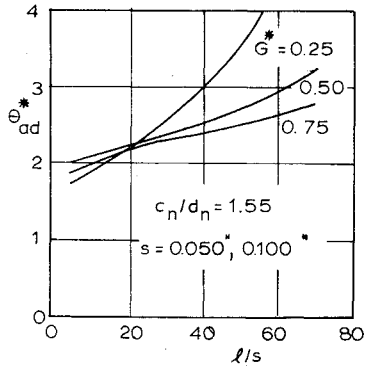

Fig. 10 θ^*_{ad} for c_n/d_n = 1.55, 20°.

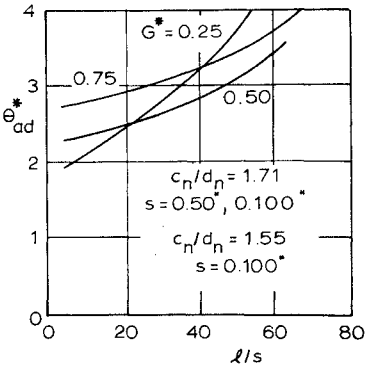

Fig. 12 θ^*_{ad} for c_n/d_n = 1.55 and 1.71, 60°.

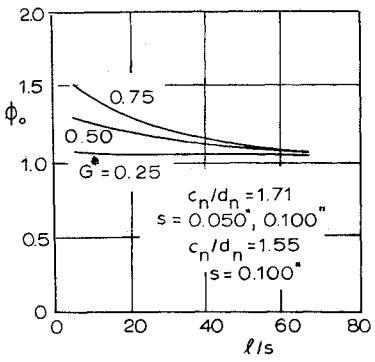

Fig. 13 Φ_0 for c_n/d_n = 1.55 and 1.71, 60°.

V. Conclusions

The reversed effect of G^* on θ^*_{ad}, apparent in the regions immediately downstream of injection, implies that not only are large injection rates wasteful of coolant, but they can actually have detrimental effects on the heat-transfer rates in these important regions.

A main conclusion of this study must be that the hole injection geometries are relatively poor from the standpoint of cooling protection offered in comparison to slot injection. The space between the holes allows the mainstream to penetrate to locations on the surface. And, as has been suggested,[9] the individual jets penetrating upward into the mainstream allow the mainstream to mix in under the jet, reducing its effectiveness. The detailed hydrodynamic and thermal features of such flows are exceedingly complex, and they deserve and will undoubtedly receive much more attention in the future. In the interim period, it is hoped that the results of this study will aid the designer in evaluating alternative film injection configurations.

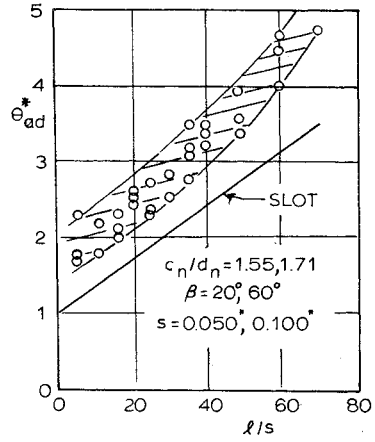

Fig. 14 θ^*_{ad} for hole injection at G^* = 0.5.

References

[1] Scesa, S., "Effect of Local Normal Injection on Flat Plate Heat Transfer," Ph.D. thesis, Univ. of California, Berkeley, Calif. 1954.

[2] Hartnett, J. P., Birkebak, R. C., and Eckert, E. R. G., "Velocity Distributions, Effectiveness, and Heat Transfer for Air Injected Through A Tangential Slot Into a Turbulent Boundary Layer," *Journal of Heat Transfer, Transactions of the American Society of Mechanical Engineers*, Vol. 83, C, 1961, pp. 293–306.

[3] Stollery, J. L., and El-Ehwany, A. A. M., "A Note on the Use of a Boundary-Layer Model for Correlating Film-Cooling Data," *International Journal of Heat and Mass Transfer*, Vol. 8, 1965, pp. 55–65.

[4] Chin, J. H. et al., "Adiabatic Wall Temperature Downstream of a Single, Tangential Injection Slot," Paper 58-A-107, American Society of Mechanical Engineers, 1958.

[5] Papell, S. S. and Trout, A. M., "Experimental Investigation of Air Film Cooling Applied to an Adiabatic Wall by Means of an Axially Discharging Slot," TN D-9, 1959, NASA.

[6] Seban, R. A., "Heat Transfer and Effectiveness for a Turbulent Boundary Layer With Tangential Fluid Injection," *Journal of Heat Transfer, Transactions of the American Socirty of Mechanical Engineers*, Vol. 82 C, 1960, pp. 303–312.

[7] Samuel, A. E. and Joubert, P. N., "Film Cooling of an Adiabatic Flat Plate in Zero Pressure Gradient in the Presence of a Hot Mainstream and Cold Tangential Secondary Injection," *Journal of Heat Transfer, Transactions of the American Society of Mechanical Engineers*, Vol. 87 C, 1965, pp. 409–418.

[8] Wieghardt, K., "Hot Air Discharge for De-Icing," A.A.F. translation F-TS-919-RE, 1946.

[9] Goldstein, R. J., Eckert, E. R. G., and Ramsey, J. W., "Film Cooling With Injection Through Holes: Adiabatic Wall Temperatures Downstream of a Circular Hole," *Journal of Engineering for Power, Transactions of the American Society of Mechanical Engineers*, Vol. 90 A, 1968, pp. 384–395.

[10] Metzger, D. E., Carper, H. J., and Swank, L. R., "Heat Transfer With Film Cooling Near Non-Tangential Injection Slots," *Journal of Engineering for Power, Transactions of the American Society of Mechanical Engineers*, Vol. 90 A, 1968, pp. 157–163.

[11] Fletcher, D. D., "The Chordwise Variation in Heat Transfer With Film Cooling Near Non-Tangential Injection Slots and Holes," M.S. thesis, 1968, Arizona State University, Tempe, Ariz.

[12] Kline, S. J. and McClintock, F. A., "Describing Uncertainties in Single-Sample Experiments," *Mechanical Engineering*, Vol. 75, Jan. 1953, p. 3.